Psychological Medicine

cambridge.org/psm

A comprehensive hierarchical comparison of structural connectomes in Major Depressive Disorder cases *v.* controls in two large population samples

Gladi Thng[1], Xueyi Shen[1], Aleks Stolicyn[1], Mark J. Adams[1], Hon Wah Yeung[1], Venia Batziou[2], Eleanor L. S. Conole[3,4], Colin R. Buchanan[4,5,6], Stephen M. Lawrie[1], Mark E. Bastin[4,6], Andrew M. McIntosh[1,3,7], Ian J. Deary[4,5], Elliot M. Tucker-Drob[8,9], Simon R. Cox[4,5,6], Keith M. Smith[10], Liana Romaniuk[1] and Heather C. Whalley[1,3,7]

[1]Division of Psychiatry, Centre for Clinical Brain Sciences, University of Edinburgh, Edinburgh, UK; [2]Edinburgh Medical School: Biomedical Sciences, University of Edinburgh, Edinburgh, UK; [3]Centre for Genomic and Experimental Medicine, Institute of Genetics and Cancer, University of Edinburgh, Edinburgh, UK; [4]Lothian Birth Cohorts, University of Edinburgh, Edinburgh, UK; [5]Department of Psychology, University of Edinburgh, Edinburgh, UK; [6]Scottish Imaging Network, A Platform for Scientific Excellence Collaboration (SINAPSE), Edinburgh, UK; [7]Generation Scotland, Institute of Genetics and Cancer, University of Edinburgh, Edinburgh, UK; [8]Department of Psychology, University of Texas, Austin, TX, USA; [9]Population Research Center and Center on Aging and Population Sciences, University of Texas, Austin, TX, USA and [10]Department of Computer and Information Sciences, University of Strathclyde, Glasgow, UK

Original Article

Cite this article: Thng G *et al* (2024). A comprehensive hierarchical comparison of structural connectomes in Major Depressive Disorder cases *v.* controls in two large population samples. *Psychological Medicine* **54**, 2515–2526. https://doi.org/10.1017/S0033291724000643

Received: 20 July 2023
Revised: 14 January 2024
Accepted: 23 February 2024
First published online: 18 March 2024

Keywords:
big data; depression; graph theory; hierarchical; MDD; network; structural connectome

Corresponding author:
Gladi Thng;
Email: J.G.Thng@sms.ed.ac.uk

Abstract

Background. The brain can be represented as a network, with nodes as brain regions and edges as region-to-region connections. Nodes with the most connections (hubs) are central to efficient brain function. Current findings on structural differences in Major Depressive Disorder (MDD) identified using network approaches remain inconsistent, potentially due to small sample sizes. It is still uncertain at what level of the connectome hierarchy differences may exist, and whether they are concentrated in hubs, disrupting fundamental brain connectivity.

Methods. We utilized two large cohorts, UK Biobank (UKB, $N = 5104$) and Generation Scotland (GS, $N = 725$), to investigate MDD case–control differences in brain network properties. Network analysis was done across four hierarchical levels: (1) global, (2) tier (nodes grouped into four tiers based on degree) and rich club (between-hub connections), (3) nodal, and (4) connection.

Results. In UKB, reductions in network efficiency were observed in MDD cases globally ($d = -0.076$, pFDR = 0.033), across all tiers ($d = -0.069$ to -0.079, pFDR = 0.020), and in hubs ($d = -0.080$ to -0.113, pFDR = 0.013–0.035). No differences in rich club organization and region-to-region connections were identified. The effect sizes and direction for these associations were generally consistent in GS, albeit not significant in our lower-N replication sample.

Conclusion. Our results suggest that the brain's fundamental rich club structure is similar in MDD cases and controls, but subtle topological differences exist across the brain. Consistent with recent large-scale neuroimaging findings, our findings offer a connectomic perspective on a similar scale and support the idea that minimal differences exist between MDD cases and controls.

Introduction

Brain regions are linked together by white matter tracts formed from bundles of axonal fibers that facilitate information transfer from one region to another (Sporns, 2011). As brain function is constrained to a certain extent by anatomical connections (Suárez, Markello, Betzel, & Misic, 2020), variations in these pathways may contribute to changes in brain function. Studies have reported subtle reductions in the fractional anisotropy (FA; a measure of the coherence of axonal fibers) of multiple individual white matter tracts in Major Depressive Disorder (MDD; Chen et al., 2016; van Velzen et al., 2020), thus hinting at reduced structural connectivity. However, since the brain is organized as a network (regions as nodes, connections as edges), the use of network approaches, such as graph theory (Sporns, 2018) and network-based statistics (Zalesky, Fornito, & Bullmore, 2010), is better suited to study structural

© The Author(s), 2024. Published by Cambridge University Press. This is an Open Access article, distributed under the terms of the Creative Commons Attribution licence (http://creativecommons.org/licenses/by/4.0/), which permits unrestricted re-use, distribution and reproduction, provided the original article is properly cited.

differences present in MDD as they can provide information on topological organization in addition to connectivity strength. This will add to the insights that can be gained by studying individual regions in isolation.

Multiple studies have since examined MDD case–control differences in brain network architecture across different scales, at the global (network-wide), nodal (individual nodes), and connection (individual edges) levels (Gong & He, 2015; Yun & Kim, 2021). Differences were generally not found at the global level but at the nodal and connection levels (Sacchet, Prasad, Foland-Ross, Thompson, & Gotlib, 2015; Xu et al., 2021). For example, MDD cases had lower clustering coefficient (i.e. the extent to which nodes are clustered together) for regions involved in the cognitive-emotion circuitry (Qin et al., 2014) and reduced connectivity in subnetworks involving regions in the default mode network (DMN; Korgaonkar, Fornito, Williams, & Grieve, 2014). While there is a consensus that connectomic differences do exist in MDD, there is currently no unanimity regarding specific differences due to lack of replication. Large sample sizes are needed to ensure the accurate estimation of effect sizes (Button et al., 2013; Grady, Rieck, Nichol, Rodrigue, & Kennedy, 2021; Marek et al., 2022; Poldrack et al., 2017) but previous studies were limited by small sample sizes (mostly $N < 100$; Xu et al., 2021). In the context of a highly prevalent and heterogeneous disorder like MDD (Fried & Nesse, 2015), results from small-scale studies may not be generalizable to the wider population too. As with large neuroimaging studies (e.g. UK Biobank) that have contributed robust findings on brain structural differences associated with MDD (Anderson et al., 2020; van Velzen et al., 2020), it is of interest to leverage these large cohorts for connectomic studies as well.

One of the features that differentiates brain networks from random networks is the presence of hubs (regions with high degree of connectivity). The concept of rich club organization suggests that hubs are densely interconnected with one another to form a rich core that functions as the central backbone of brain communication (van den Heuvel & Sporns, 2011; van den Heuvel & Sporns, 2013; van den Heuvel, Kahn, Goñi, & Sporns, 2012). It has been proposed that aberrant functioning of the network, as seen in neurological and psychiatric disorders (Crossley et al., 2014; Warren et al., 2014), is due to disruptions in the connectivity of hubs. For instance, computationally simulated attacks on rich club connections were shown to impair global network efficiency (i.e. efficiency of information exchange) to a greater extent as compared to random attacks on non-rich club connections (van den Heuvel & Sporns, 2011). Given the global impact that the disruption of the rich core has, it is possible that the rich core may be affected in MDD, which is characterized by a wide range of cognitive, affective, and somatic symptoms. At the same time, the importance of non-hubs was highlighted in a study investigating the complexity of connectivity patterns of nodes (i.e. how similar were the connections established by nodes of the same degree, in terms of the degrees of nodes they were connected to; Smith et al., 2019). Nodes were divided into node tiers based on node degrees, with the first tier comprising nodes in the top 25% of degrees, and so on. It was reported that the most complex nodes were found in the lower tiers, while nodes in the highest tier (hubs) were the least complex. The wide variability in connectivity patterns of non-hubs play an important role in bridging nodes across different tiers, which is needed to support the diverse functional roles of the brain. As such, disruptions at non-hubs may affect cross-tier connectivity and play a significant role in disease etiology, possibly even more so than disruption of hubs. This, however, requires further testing. Given the above, it is of benefit to investigate the differences in the connectivity of hubs alongside non-hubs to determine key associations with MDD.

In summary, MDD is a complex disorder that is associated with structural differences in the brain network. To date, attempts to understand these associations from a connectomic perspective have been limited by small sample sizes and consequent low statistical power. Due to the lack of consensus on the regions implicated in MDD, specifically the involvement of hubs and non-hubs, the neurobiological associations of MDD remain uncertain. Thus, the goal of this study is to utilize two large adult population samples to investigate MDD case–control differences in the structural connectome using network-based methods. To this end, we adopted a comprehensive approach of making comparisons at the global, tier, nodal, and connection level to tease out MDD-associated differences at each hierarchical level of the connectome (Fig. 1).

Methods

Participants

The discovery sample consisted of participants that were part of the first 10 000 brain imaging datasets from the UK Biobank (UKB) study (Sudlow et al., 2015). The study was approved by the National Health Service Research Ethics Service (No. 11/NW/0382) and the UK Biobank Access Committee (Project No. 4844 and 10279). All participants provided informed consent. Participants were excluded if they had (1) neurological conditions including multiple sclerosis and Parkinson's disease, (2) other mental health conditions including bipolar disorder and post-traumatic stress disorder, and (3) failed neuroimaging quality control as detailed in an earlier publication (Buchanan et al., 2020). The final sample comprised $N = 5104$ subjects with both MDD and imaging data (Table 1). The replication sample consisted of participants from the imaging subsample of the Generation Scotland: the Scottish Family Health Study (GS; Habota et al., 2021). GS received ethical approval from the NHS Tayside research ethics committee. All participants provided informed consent (reference 14/SS/0039). The same exclusion criteria as UKB were applied, and the final sample comprised $N = 725$ subjects with both MDD and imaging data (Table 1). Details on recruitment and assessments for both samples have been provided elsewhere (Alfaro-Almagro et al., 2018; Miller et al., 2016) and in the supplementary materials.

Derivation of structural connectomes

Structural connectome processing was done locally and harmonized across UKB and GS using the same procedure published previously (Buchanan et al., 2020). Each T1-weighted image was parcellated into 85 neuroanatomical regions-of-interest (ROI). Eight subcortical structures per hemisphere (accumbens area, amygdala, caudate nucleus, hippocampus, pallidum, putamen, thalamus, and ventral diencephalon), and the brainstem were extracted with FreeSurfer v5.3.0, and 34 cortical structures per hemisphere were identified using the Desikan-Killany atlas (Desikan et al., 2006). Probabilistic tractography (BEDPOSTX/ProbtrackX; Behrens, Berg, Jbabdi, Rushworth, & Woolrich, 2007; Behrens *et al.*, 2003) was performed and streamlines were seeded from all white matter voxels. Networks were constructed by identifying pairwise connections between the 85 ROIs and

https://doi.org/10.1017/S0033291724000643 Published online by Cambridge University Press

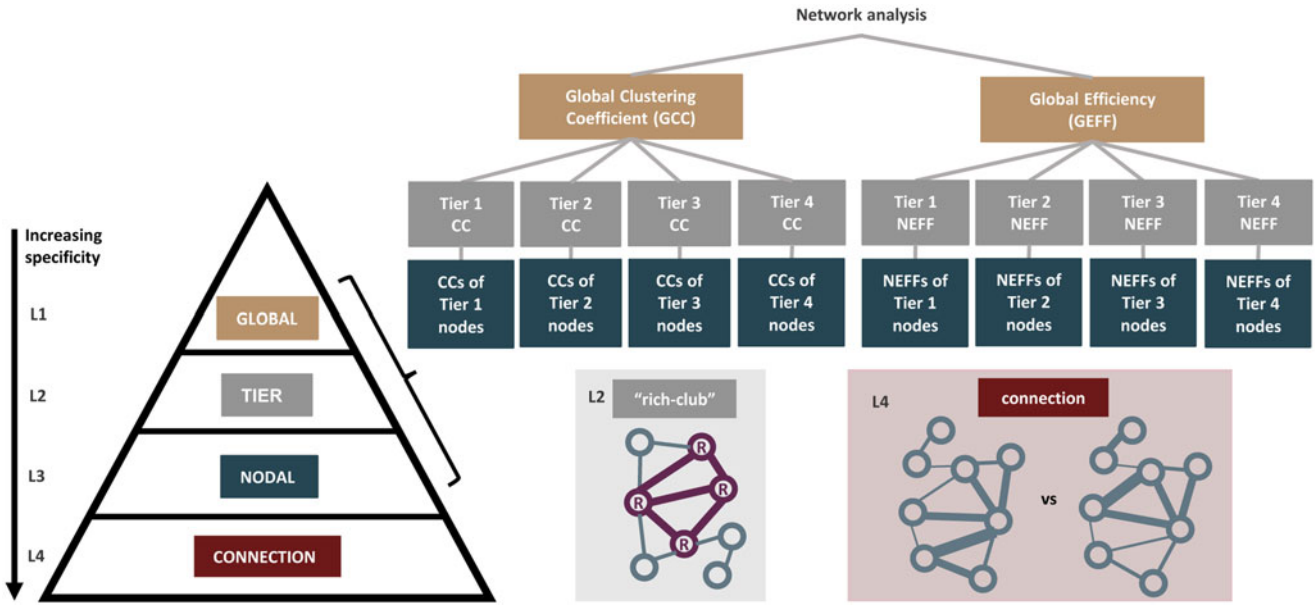


Figure 1. An overview of how the hierarchical order was established. We compared the structural connectomes of MDD cases and healthy controls in a hierarchical manner from levels 1 to 4 (L1–L4), in the order of increasing specificity. At the global network-wide level at L1, network measures including global clustering coefficient (GCC) and global efficiency (GEFF) were derived. At L2, the nodes were then grouped into four tiers based on their node degrees and tier-level network measures were compared. The presence of rich club organization looking at hub-to-hub connections was also separately studied at L2. At L3, network measures including clustering coefficient (CC) and nodal efficiency (NEFF) for each individual node were derived. At L4, Network-Based Statistics (NBS) was used to identify case–control group differences at the level of individual region-to-region connections.

represented in the form of 85×85 matrices. FA-weighted matrices were derived by recording the mean FA along interconnecting streamlines between each pair of nodes. Given that raw networks contain many false-positive connections (Thomas et al., 2014), density-based thresholding was used to retain the top x% of strongest edges for each subject's connectome (Rubinov & Sporns, 2010), on the assumption that connections with the lowest weights are spurious and differ according to individuals. Seven thresholds ranging from 10% to 40% were applied. To select the main threshold, we took the case–control Cohen's d for all global, tier, and nodal network measures, and calculated the correlation between those derived in UKB and those derived in GS. A higher correlation coefficient implies that the results between both cohorts are more agreeable, vice versa. The threshold of 35% with the strongest correlation ($r_s = 0.37$, $p = 7.1 \times 10^{-7}$) was selected to be reported here. Of note, the correlation coefficient at other thresholds was also similar (online Supplementary Fig. S1), suggesting that the replication results were consistent and there is no bias in the selection of the main threshold. This is in line with previous studies which considered similar thresholds (Buchanan et al., 2020).

MDD status

Lifetime MDD status in UKB and GS was determined using online questionnaires based on the Composite International Diagnostic Interview Short Form (CIDI; Kessler, Andrews, Mroczek, Ustun, & Wittchen, 1998). To fulfil criteria for MDD, cases were defined as ever having at least one core symptom of depression (prolonged sadness, loss of interest) for the majority or all days over a two-week period, and at least four non-core depressive symptoms (tiredness, weight change, sleep change, concentration difficulty, feeling worthless, thoughts of death) during the same period. Controls were subjects who did not endorse depression and did not screen positive for CIDI. Further details on how the case–control status was defined can be found here (Davis et al., 2020).

Network measures (L1: global; L3: nodal)

Four edge-weighted measures (two global, two nodal) focusing on clustering and efficiency were derived for each subject. The clustering coefficient (CC) measures the fraction of neighbors of the node that are also connected with each other. The weighted CC is the geometric average of the weights of the links forming all closed triplets centered on the node (Onnela, Saramäki, Kertész, & Kaski, 2005). The global clustering coefficient (GCC) gives an overall indication of the clustering in the network and is defined as the average of all CCs. The nodal efficiency (NEFF) measures how well a node is integrated within the network via its shortest paths. It is the sum of the reciprocals of the shortest path lengths from the node to all other nodes of the network (Latora & Marchiori, 2001). The global efficiency (GEFF) measures the efficiency of information exchange in which nodes concurrently exchange information via their shortest paths. It is defined as the average of all NEFFs.

The focus on CC and efficiency measures is because the human brain is postulated to be a 'small-world' network characterized by high CC and short path lengths. In other words, nodes are highly connected together through a small number of steps to ensure a high rate of information transfer to support complex brain functions at a low energy cost. Given that the small-network topology is already evident during the early developmental years (Fan et al., 2011), it is thus of interest to see if these fundamentally important network measures are affected in MDD.

https://doi.org/10.1017/S0033291724000643 Published online by Cambridge University Press

Table 1. Demographic information of participants from UKB and GS

	UKB			GS		
	Cases	Controls	*p* Value	Cases	Controls	*p* Value
Sample size (% of cohort)	1505 (29%)	3599 (71%)	–	132 (18%)	593 (82%)	–
Age	60 ± 7	63 ± 7	<0.0001	57 ± 10	60 ± 10	0.004
Sex (% female)	67.1	47.3	<0.0001	80.3	56.3	<0.0001
Education (% of group)			0.651			0.844
College or university	78 (6%)	197 (6%)		–	–	
A-levels or AS levels or equivalent	74 (5%)	195 (6%)		–	–	
O-levels or GCSEs or equivalent	82 (6%)	125 (4%)		–	–	
CSEs or equivalent	294 (21%)	691 (21%)		–	–	
NVQ or HND or HNC or equivalent	216 (15%)	487 (15%)		–	–	
Other professional qualifications (e.g. nursing, teaching)	660 (47%)	1605 (48%)		–	–	
Compulsory	–	–		24 (18%)	138 (23%)	
More than compulsory	–	–		57 (43%)	204 (35%)	
Post secondary	–	–		51 (39%)	251 (42%)	
Household income (% of group)			<0.001			0.003
Greater than £100 000	211 (15%)	348 (11%)		–	–	
£52 000 to £100 000	326 (24%)	752 (23%)		–	–	
£31 000 to £51 999	422 (31%)	992 (31%)		–	–	
£18 000 to £30 999	342 (25%)	893 (28%)		–	–	
Less than £18 000	69 (5%)	228 (7%)		–	–	
More than £70 000	–	–		11 (10%)	92 (18%)	
Between £50 000 and £70 000	–	–		7 (6%)	99 (19%)	
Between £30 000 and £50 000	–	–		36 (33%)	154 (30%)	
Between £10 000 and £30 000	–	–		48 (44%)	161 (31%)	
Less than £10 000	–	–		8 (7%)	15 (2%)	

GCSE, General Certificate of Secondary Education; CSE, Certificate of Secondary Education; NVQ, National Vocational Qualification; HND, Higher National Diploma; HNC, Higher National Certificate.
Note: *p* values represent differences between cases and controls.

Tier-based network measures (L2)

For each individual network, four node tiers were defined based on node degrees, using the method by Smith et al. (2019). Tier 1 (T1) comprised nodes in the top 25% according to their degrees (i.e. hubs), Tier 2 (T2) comprised nodes in the next 25%, and so on for Tier 3 (T3) and Tier 4 (T4). The tiers were defined separately for each subject, as nodes may have different degrees and belong to different tiers in different subjects. For each subject and each nodal measure, measures for each tier (e.g. T1_CC, T1_NEFF) were derived by averaging the measure values of all nodes in the respective tiers.

This tier-based analysis is particularly interesting given that earlier studies showed that both neonatal and adult structural connectomes are composed of distinct hierarchical tiers, with different tiers comprising different categories of functional processing (Blesa et al., 2021). By dividing nodes into tiers, we are able to assess if there are any tiers that are particularly affected in MDD (e.g. hubs in T1 *v.* non-hubs in other tiers) and are possibly driving the effects observed at the global level.

Rich club organization (L2)

A rich club organization is present when high degree nodes are more likely to be interconnected and have stronger connection among themselves than would occur by chance (Opsahl, Colizza, Panzarasa, & Ramasco, 2008). Group-averaged networks were used to calculate the weighted rich club coefficient, $\Phi(k)$. All non-zero connections were first ranked according to their weight (W^{rank}). For each degree k, a sub-graph comprising nodes with a degree larger than k was selected. The number of connections ($E_{>k}$) present between nodes in the sub-graph and the sum of their weights ($W_{>k}$) were determined. $\Phi(k)$ was then defined as the ratio between $W_{>k}$ and the sum of the top $E_{>k}$ links in the entire network (Equation 1).

$$\Phi(k) = \frac{W_{>k}}{\sum_{l=1}^{E_{>k}} w_l^{\text{rank}}} \quad (1)$$

To ensure that these high degree nodes are not interconnected due to chance, 1000 random networks (with weights randomly

https://doi.org/10.1017/S0033291724000643 Published online by Cambridge University Press

reassigned while preserving the binary topology) were generated for each k and a corresponding $\Phi_{rand}(k)$ was calculated by averaging all 1000 random networks. A normalized rich club coefficient $\Phi_{norm}(k)$ was derived as the ratio of $\Phi(k)$ over $\Phi_{rand}(k)$. A $\Phi_{norm}(k)$ of greater than 1 over a continuous range of k would suggest the existence of rich club organization.

Network-based statistics (NBS; L4)

NBS (v1.2; Zalesky et al., 2010) was used to test for differences in strength of each region-to-region connection. It evaluates the null hypothesis at the level of subnetworks instead of individual connections, with the assumption that connections associated with the effect of interest are likely to be connected. A two-sample t test was first performed to test for reduced connectivity in MDD cases at every connection, controlling for age and sex (and site for GS). A component-forming threshold of $p < 0.05$ was used to select a set of suprathreshold edges, and all connected subnetworks at this level were identified. To evaluate the significance of the subnetwork, permutation testing was done by shuffling group membership (5000 permutations) to obtain a null distribution of maximal subnetwork sizes. The p value was defined as the proportion of permutations for which the largest subnetwork was of the same size or greater ($p < 0.05$, FWE-corrected for comparison of multiple subnetworks).

Statistical analysis

The significance of (1) rich club curves for MDD cases and controls, and (2) case–control differences in rich club organization were tested using permutation testing. (1) For each degree k, the 1000 generated random networks produced a null distribution of rich club coefficients. Using this distribution, a p value was assigned to the $\Phi_{norm}(k)$ as the proportion of $\Phi_{rand}(k)$ that exceeded $\Phi_{norm}(k)$. (2) For each degree k, the differences in $\Phi_{rand}(k)$ between cases and controls produced a null distribution of 1000 differences. Using this distribution, a p value was assigned to each case–control difference in $\Phi_{norm}(k)$ as the proportion of random differences that exceeded the observed difference. FDR correction was applied and significance was determined at pFDR<0.05.

Linear regression was used to assess case–control differences in network measures, controlling for age, sex, and site (for GS only which had two sites; UKB had one site). The t-values for the group factor were used to compute Cohen's d effect sizes (Nakagawa & Cuthill, 2007). Permutation testing used to assess significance was done by shuffling group membership to obtain a null distribution of t-values for the group factor (1000 permutations). The p value was defined as the proportion of permutations for which the unsigned t-value was greater than the original unsigned t-value. Given the hierarchical structure of the data (Fig. 1), hierarchical FDR correction (Yekutieli, 2008) was performed. FDR correction was first applied across all global measures. For measures that remained significant, FDR correction was then applied across all measures at next level belonging to the same family (e.g. if GEFF remains significant, FDR correction will then be applied across all tier-based NEFFs). This process was repeated for the last level (nodal). Significance was determined at pFDR<0.05.

As sensitivity analysis, we controlled for additional covariates, including education level, household income, and body mass index. To ensure that the effects were not driven by antidepressant exposure, we also tested for differences between (1) MDD cases with and without antidepressant use, and (2) MDD cases without antidepressant use and controls. The list of antidepressants is listed in online Supplementary Table S2.

Results

Global level

GEFF ($d = -0.076$, pFDR = 0.033) was significantly lower in MDD cases in UKB (Fig. 2a, online Supplementary Table S3). The effect size was similar in GS and in the same direction, however differences did not reach significance after FDR correction potentially due to reduced power on basis of smaller sample size ($d = -0.108$, $p = 0.246$, pFDR = 0.737; online Supplementary Table S4). GCC in UKB was non-significant after FDR correction ($d = -0.058$, pFDR = 0.051) and the effect size was not replicated in GS ($d = -0.007$, $p = 0.937$, pFDR = 0.937). As post-hoc analysis, we looked at case–control differences in (1) mean FA which represents the mean weight used to construct the weighted network measures, and (2) GEFF after controlling for mean FA. No significant differences in mean FA were observed (UKB: $d = -0.012$, $p = 0.704$; GS: $d = -0.033$, $p = 0.734$), and GEFF remained significant with similar effect sizes after controlling for mean FA (UKB: $d = -0.076$, $p = 0.014$; GS: $d = -0.104$, $p = 0.283$).

Tier level

Tier membership of nodes was highly consistent between cases and controls within each cohort (UKB: $r_s = 0.991$; GS: $r_s = 0.740$) and were similar between cohorts (cases: $r_s = 0.842$; controls: $r_s = 0.842$) (Fig. 2b). T1 corresponds to the rich club and it consists of regions involved in higher-order brain functions such as the thalamus, putamen, precuneus, superior frontal gyrus, and superior parietal cortex (based on results in UKB). NEFF of all tiers were significantly lower in MDD cases (T1: $d = -0.076$, pFDR = 0.020; T2: $d = -0.069$, pFDR = 0.020; T3: $d = -0.075$, pFDR = 0.020; T4: $d = -0.079$, pFDR = 0.020; Fig. 2c) and the above effect sizes were well-replicated in GS, albeit non-FDR-significant (T1: $d = -0.108$, $p = 0.312$, pFDR = 0.416; T2: $d = -0.097$, $p = 0.306$, pFDR = 0.416; T3: $d = -0.075$, $p = 0.429$, pFDR = 0.429; T4: $d = -0.123$, $p = 0.205$, pFDR = 0.416; Fig. 2c). Effect sizes for CC tier-based measures were less consistent between cohorts. Given the hierarchical structure of the data, significance of CC tier-based measures after multiple correction was not tested due to GCC not reaching significance.

Rich club organization

Both cases and controls in UKB exhibited rich club organization, as $\Phi_{norm}(k)$ were greater than one over a range of degree k ($k = 13$ to $k = 63$, pFDR<0.005) (Fig. 3a and 3b). Similar results were observed in GS (online Supplementary Fig. S2). In UKB, significant case–control differences were observed at $k = 16$, $k = 23$, and $k = 24$ (pFDR = 0.017–0.027; Fig. 3c). However, these degree thresholds do not implicate the rich club and the absence of significant findings at the highest degrees suggests that there are no case–control differences in rich club organization. Likewise, no significant case–control differences were found in GS at all values of degree k (pFDR<0.05, online Supplementary Fig. S2).

Nodal level

The effect sizes for CC and NEFF of all nodes were generally consistent across cohorts ($r_s = 0.30$), with cases consistently having

https://doi.org/10.1017/S0033291724000643 Published online by Cambridge University Press

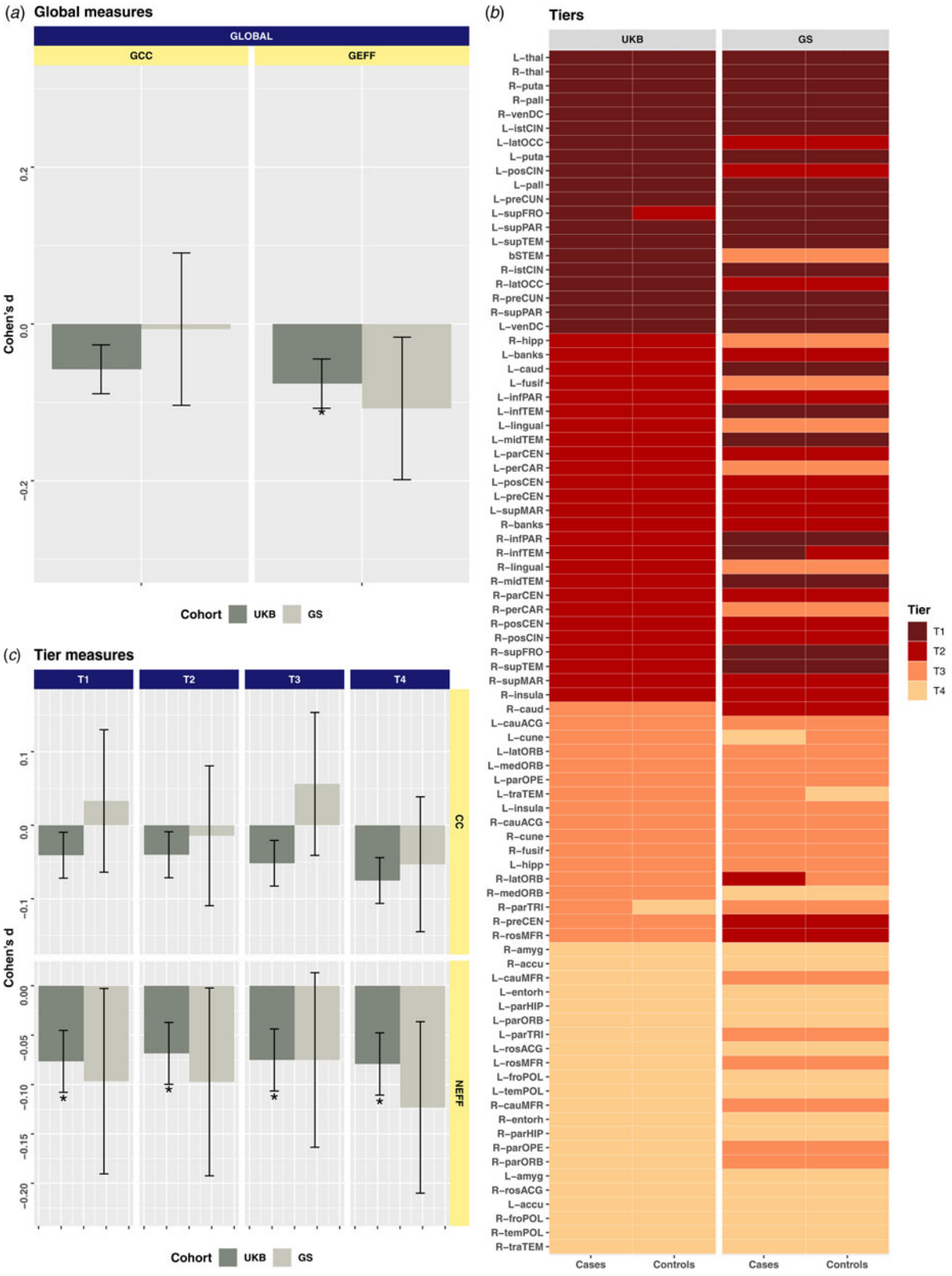


Figure 2. (a) Effect sizes for MDD case–control differences for the global network measures (GCC: global clustering coefficient; GEFF: global efficiency) for UKB and GS. The error bars represent the standard error of the estimate derived from the regression analysis. (b) All 85 nodes were ranked according to their node degree and sorted into four node tiers. T1 consists of nodes that are in the top 25% according to their degrees, and so on. To assess tier membership of nodes within each cohort, each node is assigned to the node tier that is the most dominant across all subjects in the subject group (cases or controls). (c) Effect sizes for MDD case–control differences for the tier-level network measures (tier-based CC; tier-based NEFF) for UKB and GS. The error bars represent the standard error of the estimate derived from the regression analysis. The list of nodes along with their abbreviations can be found in online Supplementary Table S1.

https://doi.org/10.1017/S0033291724000643 Published online by Cambridge University Press

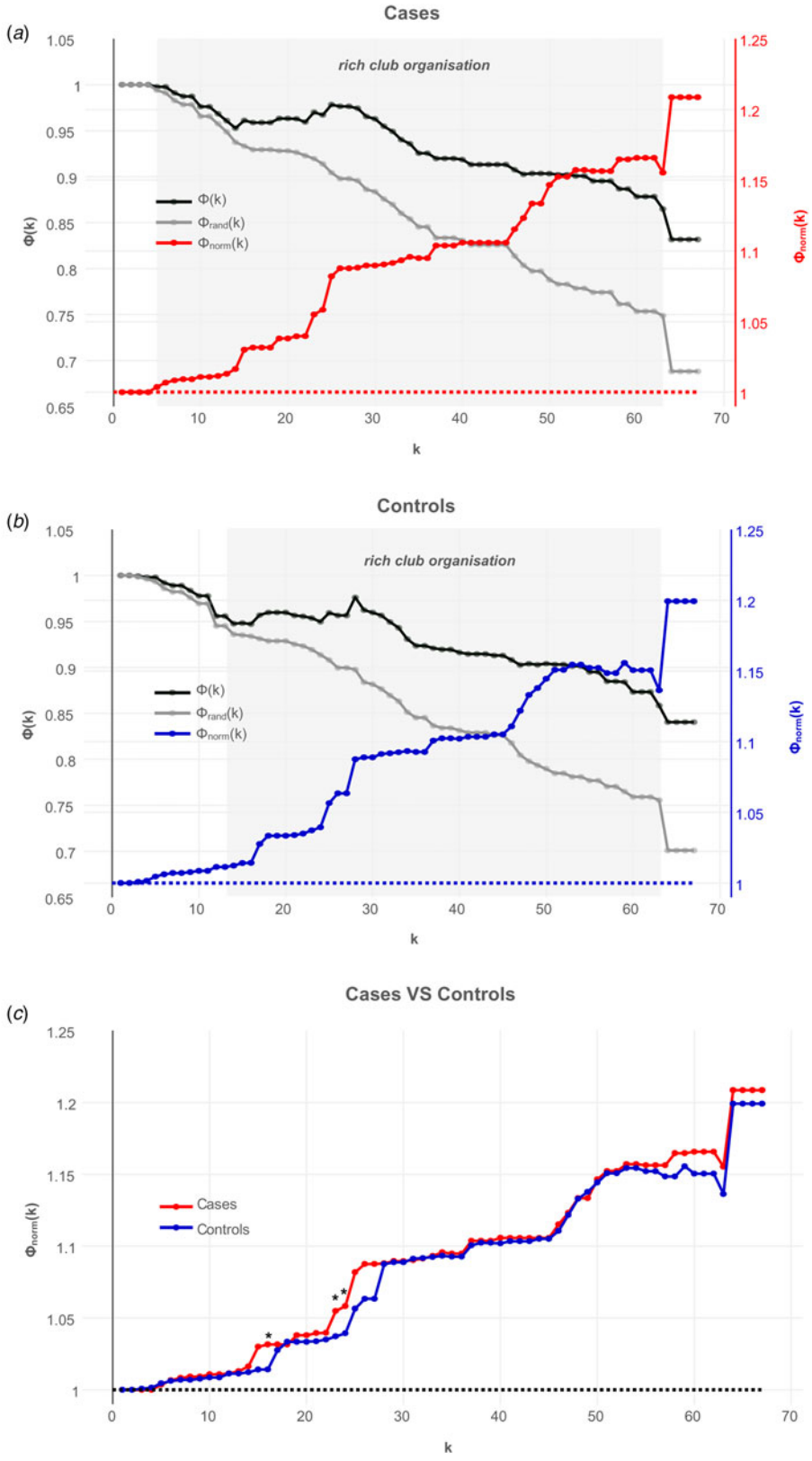


Figure 3. We tested for the presence of rich club organization (i.e. whether hubs are more likely to be interconnected and have stronger connection among themselves than would occur by chance) in (a) cases and (b) controls in UKB. For (a) and (b), the *x*-axis represents the range of degree (k) tested, the primary *y*-axis represents the rich club coefficients derived from the original network ($\Phi(k)$; black line) and the randomly generated networks ($\Phi_{rand}(k)$; grey line), and the secondary *y*-axis represents the normalized rich-club coefficients ($\Phi_{norm}(k)$; red line in (a), blue line in (b)). The shaded area represents the range of degree that showed significant rich club organization, which is indicated by a $\Phi_{norm}(k)$ of greater than 1 over a continuous range of k. A comparison of $\Phi_{norm}(k)$ for cases and controls is shown in (c).

lower values than controls (Fig. 4a and 4b). In UKB, the NEFF of nodes belonging predominantly to T1 were significantly lower in cases. These include the right thalamus ($d = -0.085$, pFDR = 0.035), right and left putamen (right: $d = -0.094$, pFDR = 0.013; left: $d = -0.099$, pFDR = 0.013), right and left pallidum (right: $d = -0.113$, pFDR = 0.013; left: $d = -0.079$, pFDR = 0.035), left precuneus ($d = -0.080$, pFDR = 0.035), left ventral diencephalon ($d = -0.080$, pFDR = 0.033), and the left insula ($d = -0.099$, pFDR

https://doi.org/10.1017/S0033291724000643 Published online by Cambridge University Press

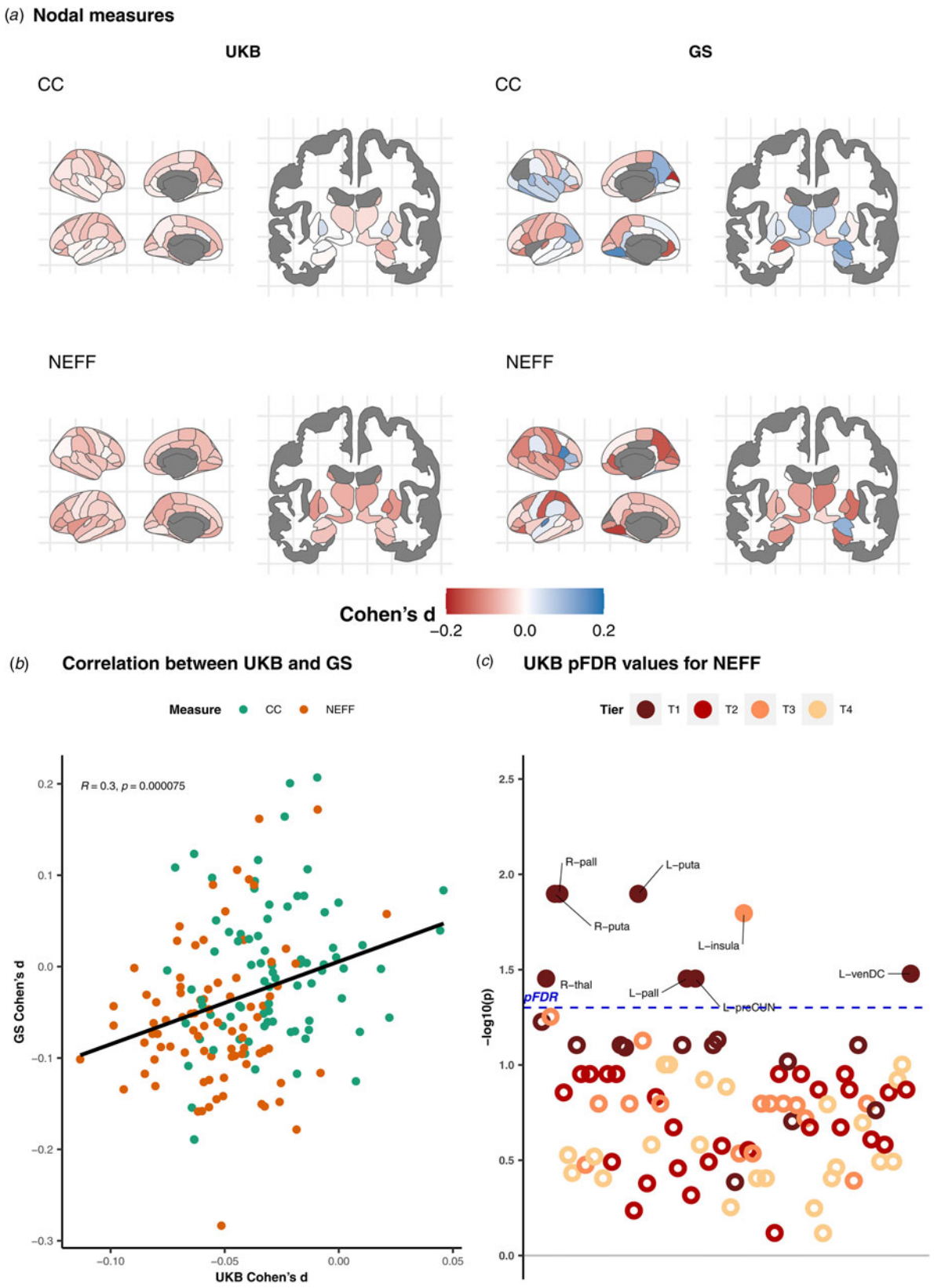


Figure 4. (a) Effect sizes for MDD case–control differences in nodal network measures (CC: clustering coefficient; NEFF: nodal efficiency) in UKB and GS. For each network measure, segmentation maps representing cortical (left) and subcortical (right) regions are shown. (b) Correlation of the effect sizes for CC and NEFF of all regions in UKB and GS. (c) FDR-corrected *p* values for the NEFF of all nodes in UKB, grouped according to their tier membership. The blue dashed line represents the significance threshold at pFDR<0.05. Filled and labelled circles represent regions that survived FDR correction.

https://doi.org/10.1017/S0033291724000643 Published online by Cambridge University Press

= 0.016) belonging to T3 (Fig. 4c). No CC measures were significantly different in both cohorts.

Connection level

No significant subnetworks were identified at the component-forming threshold of $p < 0.05$ in either UKB or GS. As recommended by the authors of NBS, the analysis was repeated at other component-forming thresholds ($p < 0.005$, $p < 0.01$, $p < 0.1$) but still no significant subnetworks were identified. As supplementary analysis, mass univariate testing for case–control differences at every connection was performed with permutation testing (50 000 times) and FDR correction applied across all tests. Again, no significant differences were found (pFDR>0.05).

Sensitivity analysis

Results at the global, tier, and nodal levels remained largely unchanged after additionally controlling for education level, household income, and body mass index (online Supplementary Tables S5–S6). Additionally, there were no significant differences between MDD cases with and without antidepressant use, suggesting that the effects of antidepressants on network measures are minimal in this sample (online Supplementary Table S7). There were no significant differences between MDD cases without antidepressant use and controls (online Supplementary Table S8), but the correlation of the effect sizes obtained here with those obtained in the main analysis was high ($r_s = 0.934$, $p < 0.001$). Given that more severe cases are likely to take medication and our samples were community-based, it is possible that the removal of cases with antidepressant use may have simultaneously removed the more severe MDD cases, thus eliminating the significance of effects. Collectively, these results show that our main findings are related to the features of MDD and not driven by antidepressant exposure.

Null results

For null findings in the main analysis and sensitivity analysis, we additionally conducted Bayes factor (BF) analysis to better understand the strength of these findings (Keysers, Gazzola, & Wagenmakers, 2020). Further information and discussion of the results derived from the BF analysis can be found in the online Supplementary Tables S9 and S10.

Discussion

This study examined the connectomic differences between MDD cases and controls in a hierarchical manner. In the discovery sample, reduction in network efficiency in MDD cases was observed globally, across all tiers, and mainly in hubs locally. No case–control differences were observed for rich club organization and at the connection level. The effect sizes were generally consistent, albeit not significant, in the smaller replication sample, which we also statistically tested in a meta-analysis (online Supplementary Fig. S3).

The reduction of global network efficiency in MDD cases suggests that there is an overall reduction in the capacity of the network to communicate between regions. Efficiency measures are based on shortest path lengths, and the brain is optimized toward a low average shortest path length to ensure efficient communication (Kaiser, Martin, Andras, & Young, 2007). As edge-weighted network measures were used, differences in efficiency could be attributed to differences in weights or topology. Given the absence of case–control differences in mean FA and the significant reduction in global efficiency in MDD even after controlling for mean FA, the differences in network efficiency may possibly be due to topological differences. The differences are, however, likely to be subtle and dispersed across the network, given that no connected subnetworks were found to be significantly different between groups at the connection level. Likewise, the inability to detect significantly different connections at the current statistical power using mass univariate testing also hints at the subtlety of effects. Nevertheless, these results are still insightful as they seem to suggest that the brain is configured slightly differently in MDD and point to the importance of studying network organization alongside connectivity strength. These topological differences can be diathetic, a sequelae, or a form of adaptation to MDD, all of which are interesting possibilities that warrant further investigation.

Interestingly, the overall reduction in network efficiency is unlikely to be associated with hub–hub connections, as indicated by the absence of significant case–control differences in rich club organization. This could be because the rich club plays a crucial role in integrating information from numerous functionally specialized regions across the brain (Kaiser et al., 2007; van den Heuvel & Sporns, 2011), and contribute toward providing a foundational basis for the development and functional specialization of lower tier regions (Blesa et al., 2021). It is arguably evolutionarily adaptive to prioritize maintaining a stable and robust core to make it resilient to changes that could critically compromise functioning. While biologically costly to maintain the rich core, the high biological cost is offset by the functional benefits it confers for neural communication (Bullmore & Sporns, 2012; Collin, Sporns, Mandl, & van den Heuvel, 2014). The manifestation of the effects of MDD in a subtle yet cumulative manner, unlike radiologically defined abnormalities that are immediately damaging, also lends support to the assertion that the rich core remains intact in MDD.

Hubs, however, may remain a key area of focus in MDD research, given that significant reductions in efficiency at the nodal level were mostly observed in T1 nodes. As rich connections between hubs have been shown above to be resilient to MDD-related changes, the differences seen in T1 may be driven by differences in feeder connections (hub to non-hub connections) instead. Hubs of interest include the thalamus, putamen, pallidum, precuneus, and ventral diencephalon, deficits which have been shown to be implicated in MDD (Kim et al., 2019; Lebedeva et al., 2017; Li, Rossbach, Zhang, Liu, & Zhang, 2018; Lu et al., 2016; Zhang et al., 2022). Of note, these regions are mostly involved in reward processing and emotion regulation. The pallidum, putamen, and thalamus are part of the cortico-basal ganglia loop, which plays a central role in developing goal-directed behaviors (Haber, 2016). Specifically, the putamen is part of the striatum (the main input structure of the basal ganglia) and receives input from various cortical structures including the anterior cingulate cortex and prefrontal cortex which comprise regions associated with reward and motivation. The pallidum, especially the ventral pallidum, is also key player in emotion processing, where it receives input from the limbic areas via the ventral striatum. Both putamen and pallidum project to the thalamus, which functions as a core information relay station from basal ganglia to the cerebral cortex and also contributes toward higher-order functions (Kumar, Beckmann, Scheffler, & Grodd,

https://doi.org/10.1017/S0033291724000643 Published online by Cambridge University Press

2022). Disruptions to this corticostriatal circuitry have been implicated in neuropsychiatric disorders including MDD (Gunaydin & Kreitzer, 2016). The precuneus and ventral diencephalon are also involved in related processes, with the former playing a central role in the DMN responsible for internally orientated cognition (e.g. rumination) and the latter containing the hypothalamus which is a key region for stress response (Zhou et al., 2020). Thus, the implication of multiple regions involved in reward/emotion regulation processes suggests that differences in this circuitry may be more important in MDD (Ng, Alloy, & Smith, 2019; Park et al., 2019).

While our results point to the importance of hubs, they also suggest that hubs are not solely involved in the reduction of overall network efficiency in MDD. Reduction in tier-level efficiency was observed across all four hierarchical tiers, indicating that MDD-associated brain differences are pervasive, involving both hubs and non-hubs. Since the four tiers cover a broad set of categories of functional processing (Blesa et al., 2021; Smith et al., 2019), the widespread somatic, affective, and cognitive dysfunctions often observed in MDD may possibly be associated with changes in information flow in multiple regions belonging to different tiers. Interestingly, although MDD cases had lower efficiency at T2 to T4, there was an absence of significant findings at the nodal level for these tiers unlike for T1. This suggests that differences at these lower tiers may be a result of the accumulation of subtle reductions in the nodal efficiency of multiple nodes that were too small/insignificant to be detected individually at the nodal level. An exception would be the insula, which despite being a T3 node, also showed significant reduction in nodal efficiency. This could be due to its close proximity and connections with the abovementioned T1 nodes like the thalamus and putamen, likely necessary to support its diverse functions (including affective processes; Ghaziri et al., 2018), thus rendering its paths more susceptible to changes associated with MDD. In the same light, the significant reduction in efficiency of T1 nodes, as discussed above, is likely not attributable to large differences in only a few connections, but a result of the accumulation of subtle differences in the large number of connections surrounding it. In other words, the ability to identify significant findings in T1 nodes may be by virtue of the fact that these nodes have the highest number of connections and hence, the accumulation of more subtle differences around them.

Taking all these together, our results suggest that there are subtle, widespread, and possibly topology-related differences in the structural connectomes of MDD cases. The differences potentially build up in the order of hierarchy to effect changes that are detectable at the higher network organization levels (global, tier, and nodes in the top tier). The reasonable consistency of effect sizes in both samples suggests that the findings are likely true, although this can be determined definitively in the future using larger samples with preferably more than a thousand subjects for reliable results (Marek et al., 2022). While the small effect sizes may seem trivial, they are actually in line with recent meta-analytic and large consortia studies that found very small differences (<2% variance explained) in MDD across all neuroimaging modalities (Feng, Thompson, & Paulus, 2022; Winter et al., 2022). Our study conducted at a similar scale thus offers a connectomic perspective and provides further evidence for the notion that very subtle and potentially diffusely distributed brain-related differences exist in MDD.

While not the first to examine network measures in MDD, this study is one of the largest, well-powered, and most comprehensive hierarchical connectomic explorations of MDD to date. The use of two large samples is a strength, in that the results are generally replicable and can serve as a reliable reference for future studies. Limitations should, however, be considered. Firstly, it is known that network metrics can vary depending on various factors, such as the atlas used, thresholding method and tractography parameters, which still lack consensus in the scientific community (Adamovich, Zakharov, Tabueva, & Malykh, 2022; Wei, Cieslak, Greene, Grafton, & Carlson, 2017). Our results may thus not hold if different approaches were taken. Secondly, our results may not be directly applicable to the more severe MDD cases, as GS and UKB are community-based cohorts consisting mainly of relatively healthy individuals. Our results, however, have the benefit of better generalizability to the community and likely cover abnormalities common across different severities/subtypes, thus providing a starting point for future in-depth analyses. We considered it essential to maximize sample size by minimizing exclusions to ensure sufficient power needed to detect small effects present in MDD.

Conclusion

This study presents a comprehensive approach to the hierarchical comparison of the structural connectomes of MDD cases relative to controls in two large population cohorts. The key takeaways include (1) there is an overall reduction in network efficiency in MDD, (2) the rich club core remains robust in MDD, and (3) the connectomic differences in MDD are subtle but widespread involving both hubs and non-hubs. This work can be extended in future studies by integrating functional connectivity data (e.g. the coupling between structural and functional connectivity) to gain further insights into the basis and consequences of reduced network efficiency in MDD.

Supplementary material. The supplementary material for this article can be found at https://doi.org/10.1017/S0033291724000643.

Acknowledgements. The research was conducted using the UK Biobank resource, with approved project number 10279 and 4844. Generation Scotland received core support from the Chief Scientist Office of the Scottish Government Health Directorates (CZD/16/6) and the Scottish Funding Council (HR03006) and is currently supported by the Wellcome Trust (216767/Z/19/Z). Genotyping of the Generation Scotland samples was carried out by the Genetics Core Laboratory at the Edinburgh Clinical Research Facility, University of Edinburgh, Scotland and was funded by the Medical Research Council UK and the Wellcome Trust. This research was funded in whole, or in part, by the Wellcome Trust (ELSC: 108890/Z/15/Z; MJA: 220857/Z/20/Z). A. S. was supported through the Wellcome-University of Edinburgh Institutional Strategic Support Fund (204804/Z/16/Z) and indirectly through the Lister Institute of Preventive Medicine Award (173096). S. R. C. is supported by a Sir Henry Dale Fellowship, jointly funded by the Wellcome Trust and the Royal Society Wellcome and The Royal Society (221890/Z/20/Z). S. R. C., C. R. B., M. E. B., I. J. D., and E. M. T.-D. are supported by the US National Institutes of Health (National Institute on Aging; R01AG054628).

Competing interests. A. M. M. previously received research grant support from The Sackler Trust, as well as speaker fees from Illumina and Janssen. No potential conflicts of interest are reported for the other authors.

References

Adamovich, T., Zakharov, I., Tabueva, A., & Malykh, S. (2022). The thresholding problem and variability in the EEG graph network parameters. *Scientific Reports*, *12*(1), 18659. https://doi.org/10.1038/s41598-022-22079-2

Alfaro-Almagro, F., Jenkinson, M., Bangerter, N. K., Andersson, J. L. R., Griffanti, L., Douaud, G., … Smith, S. M. (2018). Image processing and quality control for the first 10,000 brain imaging datasets from UK Biobank. *NeuroImage*, *166*, 400–424. https://doi.org/10.1016/j.neuroimage.2017.10.034

Anderson, K. M., Collins, M. A., Kong, R., Fang, K., Li, J., He, T., … Holmes, A. J. (2020). Convergent molecular, cellular, and cortical neuroimaging signatures of major depressive disorder. *Proceedings of the National Academy of Sciences of the USA*, *117*(40), 25138–25149. https://doi.org/10.1073/pnas.2008004117

Behrens, T. E., Berg, H. J., Jbabdi, S., Rushworth, M. F., & Woolrich, M. W. (2007). Probabilistic diffusion tractography with multiple fibre orientations: What can we gain? *NeuroImage*, *34*(1), 144–155. https://doi.org/10.1016/j.neuroimage.2006.09.018

Behrens, T. E., Woolrich, M. W., Jenkinson, M., Johansen-Berg, H., Nunes, R. G., Clare, S., … Smith, S. M. (2003). Characterization and propagation of uncertainty in diffusion-weighted MR imaging. *Magnetic Resonance in Medicine*, *50*(5), 1077–1088. https://doi.org/10.1002/mrm.10609

Blesa, M., Galdi, P., Cox, S. R., Sullivan, G., Stoye, D. Q., Lamb, G. J., … Boardman, J. P. (2021). Hierarchical complexity of the macro-scale neonatal brain. *Cerebral Cortex* (*New York, N.Y.: 1991*), *31*(4), 2071–2084. https://doi.org/10.1093/cercor/bhaa345

Buchanan, C. R., Bastin, M. E., Ritchie, S. J., Liewald, D. C., Madole, J. W., Tucker-Drob, E. M., … Cox, S. R. (2020). The effect of network thresholding and weighting on structural brain networks in the UK Biobank. *NeuroImage*, *211*, 116443. https://doi.org/10.1016/j.neuroimage.2019.116443

Bullmore, E., & Sporns, O. (2012). The economy of brain network organization. *Nature Reviews. Neuroscience*, *13*(5), 336–349. https://doi.org/10.1038/nrn3214

Button, K. S., Ioannidis, J. P., Mokrysz, C., Nosek, B. A., Flint, J., Robinson, E. S., & Munafò, M. R. (2013). Power failure: Why small sample size undermines the reliability of neuroscience. *Nature Reviews. Neuroscience*, *14*(5), 365–376. https://doi.org/10.1038/nrn3475

Chen, G., Hu, X., Li, L., Huang, X., Lui, S., Kuang, W., … Gong, Q. (2016). Disorganization of white matter architecture in major depressive disorder: A meta-analysis of diffusion tensor imaging with tract-based spatial statistics. *Scientific Reports*, *6*, 21825. https://doi.org/10.1038/srep21825

Collin, G., Sporns, O., Mandl, R. C., & van den Heuvel, M. P. (2014). Structural and functional aspects relating to cost and benefit of rich club organization in the human cerebral cortex. *Cerebral Cortex* (*New York, N.Y.: 1991*), *24*(9), 2258–2267. https://doi.org/10.1093/cercor/bht064

Crossley, N. A., Mechelli, A., Scott, J., Carletti, F., Fox, P. T., McGuire, P., & Bullmore, E. T. (2014). The hubs of the human connectome are generally implicated in the anatomy of brain disorders. *Brain: A Journal of Neurology*, *137*(Pt 8), 2382–2395. https://doi.org/10.1093/brain/awu132

Davis, K. A. S., Coleman, J. R. I., Adams, M., Allen, N., Breen, G., Cullen, B., … Hotopf, M. (2020). Mental health in UK Biobank – development, implementation and results from an online questionnaire completed by 157 366 participants: A reanalysis. *BJPsych Open*, *6*(2), e18. https://doi.org/10.1192/bjo.2019.100

Desikan, R. S., Ségonne, F., Fischl, B., Quinn, B. T., Dickerson, B. C., Blacker, D., … Killiany, R. J. (2006). An automated labeling system for subdividing the human cerebral cortex on MRI scans into gyral based regions of interest. *NeuroImage*, *31*(3), 968–980. https://doi.org/10.1016/j.neuroimage.2006.01.021

Fan, Y., Shi, F., Smith, J. K., Lin, W., Gilmore, J. H., & Shen, D. (2011). Brain anatomical networks in early human brain development. *NeuroImage*, *54*(3), 1862–1871. https://doi.org/10.1016/j.neuroimage.2010.07.025

Feng, C., Thompson, W. K., & Paulus, M. P. (2022). Effect sizes of associations between neuroimaging measures and affective symptoms: A meta-analysis. *Depression and Anxiety*, *39*(1), 19–25. https://doi.org/10.1002/da.23215

Fried, E. I., & Nesse, R. M. (2015). Depression is not a consistent syndrome: An investigation of unique symptom patterns in the STAR*D study. *Journal of Affective Disorders*, *172*, 96–102. https://doi.org/10.1016/j.jad.2014.10.010

Ghaziri, J., Tucholka, A., Girard, G., Boucher, O., Houde, J. C., Descoteaux, M., … Nguyen, D. K. (2018). Subcortical structural connectivity of insular subregions. *Scientific Reports*, *8*(1), 8596. https://doi.org/10.1038/s41598-018-26995-0

Gong, Q., & He, Y. (2015). Depression, neuroimaging and connectomics: A selective overview. *Biological Psychiatry*, *77*(3), 223–235. https://doi.org/10.1016/j.biopsych.2014.08.009

Grady, C. L., Rieck, J. R., Nichol, D., Rodrigue, K. M., & Kennedy, K. M. (2021). Influence of sample size and analytic approach on stability and interpretation of brain-behavior correlations in task-related fMRI data. *Human Brain Mapping*, *42*(1), 204–219. https://doi.org/10.1002/hbm.25217

Gunaydin, L. A., & Kreitzer, A. C. (2016). Cortico-basal ganglia circuit function in psychiatric disease. *Annual Review of Physiology*, *78*, 327–350. https://doi.org/10.1146/annurev-physiol-021115-105355

Haber, S. N. (2016). Corticostriatal circuitry. *Dialogues in Clinical Neuroscience*, *18*(1), 7–21. https://doi.org/10.31887/DCNS.2016.18.1/shaber

Habota, T., Sandu, A. L., Waiter, G. D., McNeil, C. J., Steele, J. D., Macfarlane, J. A., … McIntosh, A. M. (2021). Cohort profile for the STratifying Resilience and Depression Longitudinally (STRADL) study: A depression-focused investigation of Generation Scotland, using detailed clinical, cognitive, and neuroimaging assessments. *Wellcome Open Research*, *4*, 185. https://doi.org/10.12688/wellcomeopenres.15538.2

Kaiser, M., Martin, R., Andras, P., & Young, M. P. (2007). Simulation of robustness against lesions of cortical networks. *The European Journal of Neuroscience*, *25*(10), 3185–3192. https://doi.org/10.1111/j.1460-9568.2007.05574.x

Kessler, R. C., Andrews, G., Mroczek, D., Ustun, B., & Wittchen, H. (1998). The world health organisation composite international diagnostic interview short-form (CIDI-SF). *International Journal of Methods in Psychiatric Research*, *7*(4), 171–185. https://doi.org/10.1002/mpr.47

Keysers, C., Gazzola, V., & Wagenmakers, E. J. (2020). Using Bayes factor hypothesis testing in neuroscience to establish evidence of absence. *Nature neuroscience*, *23*(7), 788–799. https://doi.org/10.1038/s41593-020-0660-4

Kim, K., Shin, J. H., Myung, W., Fava, M., Mischoulon, D., Papakostas, G. I., … Jeon, H. J. (2019). Deformities of the globus pallidus are associated with severity of suicidal ideation and impulsivity in patients with major depressive disorder. *Scientific Reports*, *9*(1), 7462. https://doi.org/10.1038/s41598-019-43882-4

Korgaonkar, M. S., Fornito, A., Williams, L. M., & Grieve, S. M. (2014). Abnormal structural networks characterize major depressive disorder: A connectome analysis. *Biological Psychiatry*, *76*(7), 567–574. https://doi.org/10.1016/j.biopsych.2014.02.018

Kumar, V. J., Beckmann, C. F., Scheffler, K., & Grodd, W. (2022). Relay and higher-order thalamic nuclei show an intertwined functional association with cortical-networks. *Communications Biology*, *5*(1), 1187. https://doi.org/10.1038/s42003-022-04126-w

Latora, V., & Marchiori, M. (2001). Efficient behavior of small-world networks. *Physical Review Letters*, *87*(19), 198701. https://doi.org/10.1103/PhysRevLett.87.198701

Lebedeva, A. K., Westman, E., Borza, T., Beyer, M. K., Engedal, K., Aarsland, D., … Haberg, A. K. (2017). MRI-based classification models in prediction of mild cognitive impairment and dementia in late-life depression. *Frontiers in Aging Neuroscience*, *9*, 13. https://doi.org/10.3389/fnagi.2017.00013

Li, G., Rossbach, K., Zhang, A., Liu, P., & Zhang, K. (2018). Resting-state functional changes in the precuneus within first-episode drug-naive patients with MDD. *Neuropsychiatric Disease and Treatment*, *14*, 1991–1998. https://doi.org/10.2147/NDT.S168060

Lu, Y., Liang, H., Han, D., Mo, Y., Li, Z., Cheng, Y., … Sun, X. (2016). The volumetric and shape changes of the putamen and thalamus in first episode, untreated major depressive disorder. *NeuroImage. Clinical*, *11*, 658–666. https://doi.org/10.1016/j.nicl.2016.04.008

Marek, S., Tervo-Clemmens, B., Calabro, F. J., Montez, D. F., Kay, B. P., Hatoum, A. S., … Dosenbach, N. U. F. (2022). Reproducible brain-wide association studies require thousands of individuals. *Nature*, *603*(7902), 654–660. https://doi.org/10.1038/s41586-022-04492-9

Miller, K. L., Alfaro-Almagro, F., Bangerter, N. K., Thomas, D. L., Yacoub, E., Xu, J., … Smith, S. M. (2016). Multimodal population brain imaging in the UK Biobank prospective epidemiological study. *Nature Neuroscience*, *19*(11), 1523–1536. https://doi.org/10.1038/nn.4393

https://doi.org/10.1017/S0033291724000643 Published online by Cambridge University Press

Nakagawa, S., & Cuthill, I. C. (2007). Effect size, confidence interval and statistical significance: A practical guide for biologists. *Biological Reviews of the Cambridge Philosophical Society*, *82*(4), 591–605. https://doi.org/10.1111/j.1469-185X.2007.00027.x

Ng, T. H., Alloy, L. B., & Smith, D. V. (2019). Meta-analysis of reward processing in major depressive disorder reveals distinct abnormalities within the reward circuit. *Translational Psychiatry*, *9*(1), 293. https://doi.org/10.1038/s41398-019-0644-x

Onnela, J. P., Saramäki, J., Kertész, J., & Kaski, K. (2005). Intensity and coherence of motifs in weighted complex networks. *Physical Review. E, Statistical, Nonlinear, and Soft Matter Physics*, *71*(6 Pt 2), 065103. https://doi.org/10.1103/PhysRevE.71.065103

Opsahl, T., Colizza, V., Panzarasa, P., & Ramasco, J. J. (2008). Prominence and control: The weighted rich-club effect. *Physical Review Letters*, *101*(16), 168702. https://doi.org/10.1103/PhysRevLett.101.168702

Park, C., Rosenblat, J. D., Lee, Y., Pan, Z., Cao, B., Iacobucci, M., & McIntyre, R. S. (2019). The neural systems of emotion regulation and abnormalities in major depressive disorder. *Behavioural Brain Research*, *367*, 181–188. https://doi.org/10.1016/j.bbr.2019.04.002

Poldrack, R. A., Baker, C. I., Durnez, J., Gorgolewski, K. J., Matthews, P. M., Munafò, M. R., … Yarkoni, T. (2017). Scanning the horizon: Towards transparent and reproducible neuroimaging research. *Nature Reviews. Neuroscience*, *18*(2), 115–126. https://doi.org/10.1038/nrn.2016.167

Qin, J., Wei, M., Liu, H., Yan, R., Luo, G., Yao, Z., & Lu, Q. (2014). Abnormal brain anatomical topological organization of the cognitive-emotional and the frontoparietal circuitry in major depressive disorder. *Magnetic Resonance in Medicine*, *72*(5), 1397–1407. https://doi.org/10.1002/mrm.25036

Rubinov, M., & Sporns, O. (2010). Complex network measures of brain connectivity: Uses and interpretations. *NeuroImage*, *52*(3), 1059–1069. https://doi.org/10.1016/j.neuroimage.2009.10.003

Sacchet, M. D., Prasad, G., Foland-Ross, L. C., Thompson, P. M., & Gotlib, I. H. (2015). Support vector machine classification of major depressive disorder using diffusion-weighted neuroimaging and graph theory. *Frontiers in Psychiatry*, *6*, 21. https://doi.org/10.3389/fpsyt.2015.00021

Smith, K., Bastin, M. E., Cox, S. R., Valdés Hernández, M. C., Wiseman, S., Escudero, J., & Sudlow, C. (2019). Hierarchical complexity of the adult human structural connectome. *NeuroImage*, *191*, 205–215. https://doi.org/10.1016/j.neuroimage.2019.02.028

Sporns, O. (2011). The human connectome: A complex network. *Annals of the New York Academy of Sciences*, *1224*, 109–125. https://doi.org/10.1111/j.1749-6632.2010.05888.x

Sporns, O. (2018). Graph theory methods: Applications in brain networks. *Dialogues in Clinical Neuroscience*, *20*(2), 111–121. https://doi.org/10.31887/DCNS.2018.20.2/osporns

Suárez, L. E., Markello, R. D., Betzel, R. F., & Misic, B. (2020). Linking structure and function in macroscale brain networks. *Trends in Cognitive Sciences*, *24*(4), 302–315. https://doi.org/10.1016/j.tics.2020.01.008

Sudlow, C., Gallacher, J., Allen, N., Beral, V., Burton, P., Danesh, J., … Collins, R. (2015). UK Biobank: An open access resource for identifying the causes of a wide range of complex diseases of middle and old age. *PLoS Medicine*, *12*(3), e1001779. https://doi.org/10.1371/journal.pmed.1001779

Thomas, C., Ye, F. Q., Irfanoglu, M. O., Modi, P., Saleem, K. S., Leopold, D. A., & Pierpaoli, C. (2014). Anatomical accuracy of brain connections derived from diffusion MRI tractography is inherently limited. *Proceedings of the National Academy of Sciences of the USA*, *111*(46), 16574–16579. https://doi.org/10.1073/pnas.1405672111

van den Heuvel, M. P., Kahn, R. S., Goñi, J., & Sporns, O. (2012). High-cost, high-capacity backbone for global brain communication. *Proceedings of the National Academy of Sciences of the USA*, *109*(28), 11372–11377. https://doi.org/10.1073/pnas.1203593109

van den Heuvel, M. P., & Sporns, O. (2011). Rich-club organization of the human connectome. *The Journal of Neuroscience*, *31*(44), 15775–15786. https://doi.org/10.1523/JNEUROSCI.3539-11.2011

van den Heuvel, M. P., & Sporns, O. (2013). Network hubs in the human brain. *Trends in Cognitive Sciences*, *17*(12), 683–696. https://doi.org/10.1016/j.tics.2013.09.012

van Velzen, L. S., Kelly, S., Isaev, D., Aleman, A., Aftanas, L. I., Bauer, J., … Schmaal, L. (2020). White matter disturbances in major depressive disorder: A coordinated analysis across 20 international cohorts in the ENIGMA MDD working group. *Molecular Psychiatry*, *25*(7), 1511–1525. https://doi.org/10.1038/s41380-019-0477-2

Warren, D. E., Power, J. D., Bruss, J., Denburg, N. L., Waldron, E. J., Sun, H., … Tranel, D. (2014). Network measures predict neuropsychological outcome after brain injury. *Proceedings of the National Academy of Sciences of the USA*, *111*(39), 14247–14252. https://doi.org/10.1073/pnas.1322173111

Wei, K., Cieslak, M., Greene, C., Grafton, S. T., & Carlson, J. M. (2017). Sensitivity analysis of human brain structural network construction. *Network Neuroscience*, *1*(4), 446–467. https://doi.org/10.1162/NETN_a_00025

Winter, N. R., Leenings, R., Ernsting, J., Sarink, K., Fisch, L., Emden, D., … Hahn, T. (2022). Quantifying deviations of brain structure and function in major depressive disorder across neuroimaging modalities. *JAMA Psychiatry*, *79*(9), 879–888. https://doi.org/10.1001/jamapsychiatry.2022.1780

Xu, S. X., Deng, W. F., Qu, Y. Y., Lai, W. T., Huang, T. Y., Rong, H., & Xie, X. H. (2021). The integrated understanding of structural and functional connectomes in depression: A multimodal meta-analysis of graph metrics. *Journal of Affective Disorders*, *295*, 759–770. https://doi.org/10.1016/j.jad.2021.08.120

Yekutieli, D. (2008). Hierarchical false discovery rate-controlling methodology. *Journal of the American Statistical Association*, *103*(481), 309–316. https://doi.org/10.1198/016214507000001373

Yun, J. Y., & Kim, Y. K. (2021). Graph theory approach for the structural-functional brain connectome of depression. *Progress in Neuro-psychopharmacology & Biological Psychiatry*, *111*, 110401. https://doi.org/10.1016/j.pnpbp.2021.110401

Zalesky, A., Fornito, A., & Bullmore, E. T. (2010). Network-based statistic: Identifying differences in brain networks. *NeuroImage*, *53*(4), 1197–1207. https://doi.org/10.1016/j.neuroimage.2010.06.041

Zhang, Y., Zhang, Y., Ai, H., Van Dam, N. T., Qian, L., Hou, G., & Xu, P. (2022). Microstructural deficits of the thalamus in major depressive disorder. *Brain Communications*, *4*(5), fcac236. https://doi.org/10.1093/braincomms/fcac236

Zhou, H. X., Chen, X., Shen, Y. Q., Li, L., Chen, N. X., Zhu, Z. C., … Yan, C. G. (2020). Rumination and the default mode network: Meta-analysis of brain imaging studies and implications for depression. *NeuroImage*, *206*, 116287. https://doi.org/10.1016/j.neuroimage.2019.116287

https://doi.org/10.1017/S0033291724000643 Published online by Cambridge University Press